effectively targeted at sites of injured vasculature where a hemostatic plug is being formed by remaining platelets in thrombocytopenia. The H12 sequence is thought to be a necessary and sufficient binding site of fibrinogen for the receptor to support optimal reactivity with platelets [16–19]. In addition, H12 peptides are known to have much higher receptor selectivity with GPIIb/IIIa as compared with that of RGD and fibrinogen, which are reactive with other integrins such as $\alpha_v\beta_3$, $\alpha_5\beta_1$ and $\alpha_M\beta_2$ expressed on blood cells including platelets and leukocytes, and vascular endothelium [8,20–22]. In fact, using CT analysis, we were able to demonstrate that, when injected intravenously into normal rats, H12-coated liposome containing iopamidol contrast dye was effectively and specifically concentrated at the site of injured vein along with skin incision of the tail (Fig. 3). Together with our series of *in vivo* observations including the present study (Fig. 4A) in which H12-coated albumin particles and liposomes displayed ability to reduce enhanced tail bleeding time in thrombocytopenic rats, the results suggest that the H12-coated product can exert hemostatic function at the vascular injury site, but not in circulation [9–11].

Our *in vivo* results clearly demonstrate the feasibility of H12-(ADP)-liposomes as a synthetic product to replace platelet transfusion for patients with thrombocytopenia. We showed that ADP encapsulation can effectively intensify the hemostatic ability of liposomes, suggesting that locally released ADP at vascular injury sites plays a significant role in primary hemostasis (Fig. 4A). A rabbit thrombocytopenia model then clearly showed that H12-(ADP)-liposomes exhibited a dose-dependent hemostatic effect as efficiently as that of fresh animal platelets (Fig. 4B). In practice, 4.0×10^9 cells kg^{-1} of platelet transfusion resulted in reduction of elongated ear bleeding time in thrombocytopenic rabbits from 1695 to 505 s, while platelet count could be corrected from 2.2×10^4 to 6.1×10^4 μL^{-1}. A nearly equivalent hemostatic effect (correction of bleeding time to 428 s) was obtained by 20 mg kg^{-1} (corresponding to 1.0×10^{13} particles kg^{-1}) of H12-(ADP)-liposome infusion. In the human setting, a standard dose of transfusion to yield clinical efficacy requires platelet concentrates containing at least 5.0×10^9 cells kg^{-1} [23]. Our rabbit model would thus simulate platelet transfusion in humans.

A major concern regarding the safety of this product involves whether enhanced platelet activation or thrombosis is induced in circulation. If ADP is recovered 100% from 20 mg kg^{-1} of H12-(ADP)-liposomes in rabbit plasma, the final ADP concentration is calculated as 5 $\mu mol\ L^{-1}$, a plasma level that would readily induce platelet activation and aggregation *in vitro* (Table 1). Local extracellular concentrations of ADP generated by maximal platelet aggregation are estimated to be around 20–30 $\mu mol\ L^{-1}$ in humans and rabbits [24]. However, the released ADP may be rapidly diluted by circulation or drastically hydrolyzed by nucleotidases present on the endothelium, leukocytes and in plasma to maintain nucleotide homeostasis [25,26]. In fact, no significant P-selectin expression (a sensitive platelet activation marker) on circulating platelets was detected in normal rabbits for 60 min after infusion of 20 mg kg^{-1} of liposome. In addition, even direct bolus infusion of extremely high concentrations of ADP (final plasma concentration, 100 $\mu mol\ L^{-1}$) did not induce P-selectin expression, suggesting that the plasma ADP catabolizing system *in vivo* is functional at least under conditions in which ADP concentrations temporarily reach the 100-$\mu mol\ L^{-1}$ range. Thus, together with the additional findings that liposome infusion had no effects on circulating platelet count (Table 1) and did not alter the plasma activity of coagulation parameters in rabbits (Table S2), our H12-(ADP)-liposomes may offer a suitable hemostatic agent that acts on activated platelets at sites of vascular injury, but not in circulation.

In conclusion, we have developed a synthetic platelet substitute comprising fibrinogen-derived H12 peptide-coated, ADP-encapsulated liposomes. As H12-(ADP)-liposomes exhibit *in vitro* function via activated platelets (Fig. 1), they seem to require endogenous platelets to work and thus may not be as effective if administered to patients with significant thrombocytopenia. At the same time, these liposomes may be useful to treat bleeding in patients with qualitative platelet disorders, such as storage pool deficiency. Further study is needed under conditions simulating various clinical settings to establish potential indications in platelet transfusion.

Acknowledgements

The authors wish to thank N. Watanabe, T. Kamata, K. Yokoyama and M. Murata at Keio University for valuable discussion and/or critical reading. This work was supported in part by Health and Labor Sciences Research Grants (Research on Public Essential Drugs and Medical Devices, S. Takeoka, Y. Ikeda and M. Handa) from the Ministry of Health, Labour and Welfare, Japan. Y. Okamura was the recipient of a research fellowship from the Japan Health Sciences Foundation.

Disclosure of Conflict of Interests

The authors state that they have no conflict of interest.

Supporting Information

Additional Supporting Information may be found in the online version of this article:

Table S1. PAC-1 binding to and P-selectin expression on platelets stirred with H12-(ADP)-liposome.
Table S2. Blood coagulation parameters in thrombocytopenic rats and rabbits after H12-(ADP)-liposome infusion.

Please note: Wiley-Blackwell are not responsible for the content or functionality of any supporting materials supplied by the authors. Any queries (other than missing material) should be directed to the corresponding author for the article.

References

1 Blajchman MA. Substitutes and alternatives to platelet transfusions in thrombocytopenic patients. *J Thromb Haemost* 2003; **1**: 1637–41.

2 Bode AP, Fischer TH. Lyophilized platelets: fifty years in the making. *Artif Cells Blood Substit Immobil Biotechnol* 2007; **35**: 125–33.
3 Agam G, Livine AA. Erythrocytes with covalently bound fibrinogen as a cellular replacement for the treatment of thrombocytopenia. *Eur J Clin Invest* 1992; **22**: 105–12.
4 Coller BS, Springer KT, Beer JH, Mohandas N, Scudder LE, Norton KJ, West SM. Thromboerythrocytes. In vitro studies of a potential autologous, semi-artificial alternative to platelet transfusion. *J Clin Invest* 1992; **89**: 546–55.
5 Andrieux A, Hudry-Clergeon G, Ryckewaert JJ, Chapel A, Ginsberg MH, Plow EF, Marguerie G. Amino acid sequences in fibrinogen mediating its interaction with its platelet receptor, GPIIbIIIa. *J Biol Chem* 1989; **264**: 9258–65.
6 Levi M, Friedrich PW, Middleton S, De Groot PG, Wu YP, Harris R, Biemond BJ, Heijien FG, Levin J, Ten Cate JW. Fibrinogen-coated albumin microcapsules reduce bleeding in severely thrombocytopenic rabbits. *Nat Med* 1999; **5**: 107–11.
7 Takeoka S, Okamura Y, Teramura Y, Watanabe N, Suzuki H, Tsuchida E, Handa M, Ikeda Y. Function of fibrinogen γ-chain dodecapeptide-conjugated latex beads under flow. *Biochem Biophys Res Commun* 2003; **312**: 773–9.
8 Ruoslahti E. RGD and other recognition sequences for integrins. *Annu Rev Cell Dev Biol* 1996; **12**: 697–715.
9 Okamura Y, Takeoka S, Teramura Y, Maruyama H, Tsuchida E, Handa M, Ikeda Y. Hemostatic effects of fibrinogen γ-chain dodecapeptide-conjugated polymerized albumin particles in vitro and in vivo. *Transfusion* 2005; **45**: 1221–8.
10 Okamura Y, Fujie T, Maruyama H, Handa M, Ikeda Y, Takeoka S. Prolonged hemostatic ability of poly(ethylene glycol)-modified polymerized albumin particles carrying fibrinogen γ-chain dodecapeptide. *Transfusion* 2007; **47**: 1254–62.
11 Okamura Y, Maekawa I, Teramura Y, Maruyama H, Handa H, Ikeda Y, Takeoka S. Hemostatic effects of phospholipid vesicles carrying fibrinogen γ-chain dodecapeptide in vitro and in vivo. *Bioconjug Chem* 2005; **16**: 1589–96.
12 Okamura Y, Fujie T, Nogawa M, Maruyama H, Handa M, Ikeda Y, Takeoka S. Hemostatic effects of polymerized albumin particles carrying fibrinogen γ-chain dodecapeptide as platelet substitutes in severely thrombocytopenic rabbits. *Transfus Med* 2008; **18**: 158–66.
13 Ware JA, Smith M, Salzman EW. Synergism of platelet-aggregating agents. Role of elevation of cytoplasmic calcium. *J Clin Invest* 1987; **80**: 267–71.
14 Cattaneo M, Canciani MT, Lecchi A, Kinlough-Rathbone RL, Packham MA, Mannucci PM, Mustard JF. Released adenosine diphosphate stabilizes thrombin-induced human platelet aggregates. *Blood* 1990; **75**: 1081–6.
15 Nishiya T, Toma C. Interaction of platelets with liposomes containing dodecapeptide sequence from fibrinogen. *Thromb Haemost* 2004; **91**: 1158–67.
16 Kloczewiak M, Timmons S, Bednarek MA, Sakon M, Hawiger J. Platelet receptor recognition domain on the γ chain human fibrinogen and its synthetic peptide analogues. *Biochemistry* 1989; **28**: 2915–9.
17 Weisel JW, Nagaswami C, Vilaire G, Bennett JS. Examination of platelet membrane glycoprotein IIb-IIIa complex and its interaction with fibrinogen and other ligands by electron microscopy. *J Biol Chem* 1992; **267**: 16637–43.
18 Farrell DH, Thiagarajan P. Binding of recombinant fibrinogen mutants to platelets. *J Biol Chem* 1994; **269**: 226–31.
19 Holmbäck K, Danton MJ, Suh TT, Daugherty CC, Degen JL. Impaired platelet aggregation and sustained bleeding in mice lacking the fibrinogen motif bound by integrin αIIbβ3. *EMBO J* 1996; **15**: 5760–71.
20 Smith JW, Ruggeri ZM, Kunicki TJ, Cheresh DA. Interaction of integrins $\alpha_v\beta_3$ and GPIIb-IIIa with fibrinogen. *J Biol Chem* 1990; **265**: 12267–71.
21 Suehiro K, Gailit J, Plow EF. Fibrinogen is a ligand for integrin $\alpha_5\beta_1$ on endothelium cells. *J Biol Chem* 1997; **272**: 5360–6.
22 Yakubenko VP, Solovjov DA, Zhang L, Yee VC, Plow EF, Ugarova TP. Identification of the binding site for fibrinogen recognition peptide γ383-395 within the α_MI-domain of integrin $\alpha_M\beta_2$. *J Biol Chem* 2001; **276**: 13995–4003.
23 Norol F, Bierling P, Roudot-Thoraval F, Le Coeur FF, Rieux C, Lavaux A, Kuentz M, Duedari N. Platelet transfusion: a dose-response study. *Blood* 1998; **92**: 1448–53.
24 Meyers KM, Holmsen H, Seachord CL. Comparative study of platelet dense granule constituents. *Am J Physiol* 1982; **243**: R454–61.
25 Heptinstall S, Johnson A, Glenn JR, White AE. Adenine nucleotide metabolism in human blood – important roles for leukocytes and erythrocytes. *J Thromb Haemost* 2005; **3**: 2331–9.
26 Atkinson B, Dwyer K, Enjyoji K, Robson SC. Ecto-nucleotidases of the CD39/NTPDase family modulate platelet activation and thrombus formation: potential as therapeutic targets. *Blood Cells Mol Dis* 2006; **36**: 217–22.

Transfusion Medicine, 2008, **18**, 158–166 doi: 10.1111/j.1365-3148.2008.00860.x

ORIGINAL ARTICLE

Haemostatic effects of polymerized albumin particles carrying fibrinogen γ-chain dodecapeptide as platelet substitutes in severely thrombocytopenic rabbits

Y. Okamura,*† T. Fujie,* M. Nogawa, ‡ H. Maruyama,§ M. Handa,† Y. Ikeda§ & S. Takeoka*

**Department of Life Science and Medical Bioscience, Graduate School of Advanced Science and Engineering, Waseda University, †Department of Transfusion Medicine & Cell Therapy, School of Medicine, Keio University, ‡Research and Development Department, Central Blood Institute, Japanese Red Cross Society, and §Department of Internal Medicine, School of Medicine, Keio University, Tokyo, Japan*

Received 25 October 2007; accepted for publication 27 March 2008

SUMMARY. Our purpose was to produce a platelet substitute that could enhance haemostatic ability using rabbits with severe thrombocytopenia. We have developed polymerized albumin particles (polyAlb) for treatment of bleeding and focused on a dodecapeptide, HHLGGAKQAGDV (H12), as a useful ligand for activated platelet. This sequence occurs only at the carboxy-terminus of the fibrinogen γ-chain (γ 400–411). H12 was conjugated to the surface of polyAlb modified with poly(ethylene glycol) (PEG) chains to produce blood-compatible particles (H12–PEG–polyAlb) that had prolonged blood residence time and enhanced stability *in vitro* and *in vivo*. The H12–PEG–polyAlb was administered intravenously to rabbits with severe thrombocytopenia, and the ear bleeding time was measured in order to evaluate the haemostatic effect. The H12–PEG–polyAlb significantly shortened the ear bleeding time of severely thrombocytopenic rabbits and showed no effect on the inhibition or promotion of endogenous and exogenous coagulation activities. Furthermore, we could assess the haemostatic capacity of the H12–PEG–polyAlb, based on the relationship between transfused platelet count and the bleeding time. The H12–PEG–polyAlb may be a suitable candidate for an alternative to human platelet concentrates infused to treat bleeding in patients with severe thrombocytopenia.

Key words: dodecapeptide (H12), ear bleeding time, PEG modification, platelet substitutes, polymerized albumin particles, thrombocytopenic rabbits.

Platelet transfusion plays an important role in supportive therapy for patients with thrombocytopenia caused by haematological malignancies or resulting from intensive chemotherapy or radiotherapy for cancer. However, the limited supply of platelet concentrates has always been a serious issue because of their short storage life (3 days in Japan), an insufficient number of donations and hence the demand that exceeds the supply. Furthermore, the risk of viral or bacterial infection associated with transfusion is also a serious issue. For these reasons, a number of trials have been conducted to develop platelet substitutes (artificial platelets) that can reproduce platelet functions, such as infusible platelet membranes (Graham *et al.*, 2001), solubilized platelet membrane protein-conjugated liposomes (plateletsomes) (Rybak & Renzulli, 1993), fibrinogen-bonded red blood cells (Agam & Livine, 1992), liposomes bearing fibrinogen (Casals *et al.*, 2003), fibrinogen-coated albumin microcapsules (Synthocytes) (Levi *et al.*, 1999) and arginyl-glycyl-aspartate (RGD) peptide-bound red blood cells (thromboerythrocytes) (Coller *et al.*, 1992). These platelet substitutes consist of materials derived from blood components.

The glycoprotein (GP) IIb/IIIa receptor on the platelet membrane is converted from an inactive to an active form when platelets adhere to collagen at the site of vascular injury (Takagi *et al.*, 2002; Xiao *et al.*, 2004). The activated GPIIb/IIIa acts as a receptor for fibrinogen and von Willebrand factor (Mustard *et al.*, 1978; Ruggeri *et al.*, 1983), and their binding is followed by platelet aggregation (De Marco *et al.*, 1986). This is because fibrinogen contains three putative binding sites for GPIIb/IIIa, namely a tetrapeptide containing an

Correspondence: Shinji Takeoka, 2-2 Wakamatsucho, Shinjuku, Tokyo, 162-8480, Japan.
Tel.: +813 5369 7324; fax: +813 5369 7324;
e-mail: takeoka@waseda.jp

RGD sequence, for example RGDF and RGDS at α 95–98 and α 572–575, respectively, and a dodecapeptide (HHLGGAKQAGDV, H12) at the γ-chain carboxy-terminal sequence (γ 400–411) (Kloczewiak *et al.*, 1982).

In order to construct platelet substitutes having the desired haemostatic effects, we have also conjugated fibrinogen (Takeoka *et al.*, 2001), recombinant platelet membrane GPIbα (Kitaguchi *et al.*, 1999; Takeoka *et al.*, 2000; Nishiya *et al.*, 2002; Takeoka *et al.*, 2002) and GPIa/IIa (Teramura *et al.*, 2003) to biocompatible and biodegradable carriers such as polymerized albumin particles (polyAlb) and phospholipid vesicles (liposomes). In particular, the fibrinogen conjugates were shown to facilitate platelet aggregation *in vitro* on an activated platelet-immobilized surface by recruiting flowing platelets into aggregates after their initial attachment (Takeoka *et al.*, 2001). However, the isolated human fibrinogen protein is not stable (Takeoka *et al.*, 2001) and tends to precipitate at 4 °C within a few hours (Wertheimer *et al.*, 1944).

Therefore, we focused on the H12 sequence instead of full-length fibrinogen (Kloczewiak *et al.*, 1982; Kloczewiak *et al.*, 1984, 1989; Lam *et al.*, 1987). The H12 conjugates showed minimal interaction with non-stimulated platelets compared with RGD conjugates, based on our results obtained from flow cytometric analyses of platelet agglutination (Takeoka *et al.*, 2003; Okamura *et al.*, 2005a). Furthermore, the H12-conjugated polyAlb enhanced the *in vitro* thrombus formation on a collagen surface, and it dose dependently reduced the tail bleeding time of rats with moderate thrombocytopenia (Okamura *et al.*, 2005b). Recently, we succeeded in prolonging the *in vivo* residence time of the H12–polyAlb by poly(ethylene glycol) (PEG) modification (H12–PEG–polyAlb) and confirmed that the H12–PEG–polyAlb haemostatic effects lasted for at least 6 h (Okamura *et al.*, 2007).

Our purpose was to produce a platelet substitute that could enhance haemostatic ability using a larger animal with severe thrombocytopenia (thrombocytopenic rabbits). In this study, the H12–PEG–polyAlb particles were administered intravenously to rabbits, and the ear bleeding time was measured to evaluate the haemostatic effect. Furthermore, we estimated the haemostatic capacity of the H12–PEG–polyAlb based on the relationship between the bleeding time and platelet transfusion.

MATERIALS AND METHODS

Reagents

Fibrinogen γ-chain dodecapeptide (C-HHLGGAKQAGDV, H12) was synthesized using a solid-phase synthesizer (BEX, Tokyo, Japan). PEGs, precisely, α-(3-[3-maleimido-1-oxopropyl]amino) propyl-ω-succinimidyl carboxypentyloxy PEG (MALPEG-NHS, molecular weight 5·0 kDa) and α-methoxy-ω-succinimidyl carboxypentyloxy PEG (mPEG-NHS, molecular weight 5·0 kDa), were purchased from NOF (Tokyo, Japan). Busulphan and PEG (average molecular weight, 400 Da) were obtained from Sigma–Aldrich (St. Louis, MO, USA). Recombinant human serum albumin (rHSA) was kindly donated by Mitsubishi Pharma (Osaka, Japan). Ketamine (60 mg mL^{-1}) and seractal 2% were purchased from Daiichi-Sankyo (Tokyo, Japan) and Bayer Medical (Tokyo, Japan), respectively. Phycoerythrin-conjugated streptavidin (PE–streptavidin) and *N*-hydroxysuccinimidobiotin (NHS–biotin) were purchased from BD-Pharmingen (San Diego, CA, USA) and Pierce Chemical (Rockford, IL, USA), respectively.

Preparation of H12–PEG–polyAlb

A suspension of polyAlb with an average diameter of 240 ± 100 nm was prepared as described previously (Okamura *et al.*, 2007). A solution of MALPEG-NHS in dimethyl sulfoxide (DMSO) (10 mM, 7·4 mL) was added to the polyAlb suspension (15 mg mL^{-1}, 250 mL), and the suspension was stirred for 20 min at room temperature. A solution of mPEG-NHS in DMSO (25 mM, 8·9 mL) was added to the suspension, and the suspension was stirred for 20 min at room temperature. The unreacted reagents and the by-products were separated by repeated centrifugation (30 000 *g*, 20 min, 4 °C, twice) and washed with phosphate-buffered saline (PBS), and MALPEG- and mPEG-modified polyAlb [(MALPEG)(mPEG)polyAlb] were collected. A suspension of (MALPEG)(mPEG)polyAlb (21 mg mL^{-1}, 70 mL) was mixed with a solution of H12 (100 mM, 292 μL) and allowed to react at room temperature for 12 h. A small molar excess of cysteine over MALPEG was added to the suspension, and the unreacted reagents were removed by repeated centrifugation (30 000 *g*, 10 min, 4 °C) and washed with PBS to obtain the purified H12-conjugated (MALPEG)(mPEG)polyAlb (H12–PEG–polyAlb, 30 mg mL^{-1}, 15 mL).

The concentrations of MALPEG, mPEG and H12 conjugated to the surface of polyAlb particles were determined by quantifying each unreacted reagent using high-pressure liquid chromatography on a TSK-GEL G3000PW_{xL} column (7·8 mM outer diameter × 300 mm height using a mobile phase of 36% acetonitrile and 0·1% trifluoroacetic acid at 1 mL min^{-1}). The unreacted reagents were detected using a reflective index detector.

Preparation of busulphan-induced thrombocytopenic rabbits

All animal studies were approved by the Animal Subject Committee of Keio University, School of Medicine, and were performed according to NIH guidelines for the care and use of laboratory animals (NIH publication 85-23 Rev. 1985). Experiments were carried out using male New Zealand white rabbits (approximately 2·5 kg, 11 weeks old; Sankyo Lab, Tokyo, Japan). The rabbits were anaesthetized by intramuscular injection of a 'cocktail' of ketamine (1·5 mL) and seractal 2% (0·5 mL). A busulphan solution was prepared at a concentration of 10 mg mL^{-1} in PEG (average molecular weight, 400 Da). After shaving the hair around the injection sites, the rabbits received a subcutaneous injection of busulphan at a dosage of 15, 20, or 25 mg kg^{-1} on days 0 and 3, to produce a total dosage of 30, 40 or 50 mg kg^{-1}, respectively. Blood samples for cell counting were withdrawn from anaesthetized rabbits by inserting a 23-gauge needle into an ear vein, and the cell counts were determined with an automated haematology analyser (K-4500; Sysmex, Kobe, Japan). To maintain adequate anaesthesia, intramuscular injection of ketamine was repeated as the need arose.

Platelet transfusion

Blood withdrawn from donor rabbits, which were anaesthetized and then exsanguinated by cardiac puncture, was mixed with a 10% volume of an acid–citrate–dextrose (ACD) solution composed of 2·2% (w/v) sodium citrate, 0·8% (w/v) citric acid and 2·2% (w/v) glucose. Platelet-rich plasma (PRP) was prepared by centrifugation (100 *g*, 15 min, 22 °C), and the resulting PRP was mixed with a 15% volume of ACD solution. The PRP was centrifuged (2200 *g*, 7 min, 22 °C), and the platelet pellet was obtained by removing the supernatant. The pellet was resuspended in platelet-poor plasma (PPP) prepared by centrifugation (2200 *g*, 10 min, 22 °C), and the platelet count was adjusted from $1{\cdot}0 \times 10^5$ per microlitre to $1{\cdot}0 \times 10^6$ per microlitre using an automated haematology analyser (K-4500). The anaesthetized rabbits with severe thrombocytopenia were cannulated on day 15 with a 23-gauge scalp vein infusion set, and the various PRPs with defined platelet counts were transfused into the ear vein by an infusion pump at a rate of 0·5 mL min^{-1} and at a dose of 4 mL kg^{-1}. Platelet recovery at 30 min was calculated as described previously (Michelson *et al.*, 1996), using an estimated blood volume of 58 mL kg^{-1} (Reimers *et al.*, 1973).

We also confirmed that the transfused platelets had a normal half-life period and survival time (The Panel on Diagnostic Application of Radioisotopes in Hematology, International Committee for Standardization in Hematology, 1977) in the blood circulation as follows: the PRP was mixed with 15% (v/v) of ACD and centrifuged (2200 *g*, 10 min, 22 °C). The plasma supernatants were replaced with a Ringer's citrate–dextrose solution [RCD solution, composition: 0·76% (w/v) citric acid, 0·090% (w/v) glucose, 0·043% (w/v) $MgCl_2$, 0·038% (w/v) KCl and 0·60% (w/v) NaCl, pH 6·5]. After resuspension, this mixture was added drop by drop to a 10 mM solution of NHS–biotin in DMSO (to a final concentration of 10 μM) and was incubated at 37 °C for 30 min. The suspension washed with the RCD solution by centrifugation (2200 *g*, 7 min, 22 °C), and the biotin-labelled PRP was resuspended to $5{\cdot}0 \times 10^5$ per microlitre in PPP prepared by centrifugation (2200 *g*, 10 min, 22 °C). Using a similar method as before, the resulting PRP was transfused into the ear vein using a 23-gauge scalp vein infusion set, and 200 μL blood was collected from the ear vein at time intervals using a 23-gauge needle. This was then mixed with ACD [final concentration 10% (v/v)], followed by centrifugation (100 *g*, 10 min, 22 °C). Ten microlitres PE–streptavidin (1 : 20 dilution of 0·5 mg mL^{-1} solution in PBS) was added to 50 μL platelet suspension, followed by incubation for 30 min at room temperature before fixing with paraformaldehyde [final concentration 1·0% (w/v)]. The platelets were gated to their characteristic forward vs. side scatter, and $1{\cdot}0 \times 10^4$ platelets were analysed using a FACS-Calibur flow cytometer (Nihon Becton Dickinson, Tokyo, Japan). The transfused platelets were quantified as a fraction of the PE-positive platelets, and the number of labelled platelets was calculated as the percentage of the circulating labelled platelets. Each experiment was performed at least three times. The platelet survival time was calculated using the 30-min recovery as 100%, as recommended by the Panel on Diagnostic Application of Radioisotopes in Hematology, International Committee for Standardization in Hematology (1977).

Measurement of the ear bleeding time

The anaesthetized thrombocytopenic rabbits were cannulated on day 15 with a 23-gauge scalp vein infusion set, and the sample suspension (10, 20 and 30 mg mL^{-1} equivalent of rHSA) was infused into the ear vein using an infusion pump at a rate of 0·5 mL min^{-1}. The samples were the H12–PEG–polyAlb and the PEG–polyAlb at a dose of 4 mL kg^{-1}, and saline was used to obtain the control value. Thirty minutes

after administration, a 6-mm-length standardized incision (No. 11 scalpel blade; AS ONE Co., Osaka, Japan) was made at a site where no vessel was visible. The ear was immersed in a saline bath, and the time until the bleeding stopped was measured. In the case of bleeding over 30 min, we registered the bleeding time as 30 min. In addition, cell counts were determined using an automated haematology analyser (K-4500) before (−5 min) and after (60 min) injection of samples.

Measurement of blood coagulation parameters

Blood withdrawn from thrombocytopenic rabbits after injection of the H12–PEG–polyAlb, the PEG–polyAlb or saline was mixed with a 10% volume of 3·8% (w/v) sodium citrate, and the plasma was collected by centrifugation (2200 *g*, 10 min, room temperature). The clinical laboratory testing such as prothrombin time (PT), activated partial thromboplastin time (APTT) and fibrinogen antigen (Fbg) was carried out by SRL, Inc. (Tokyo, Japan).

Statistical analyses

A statistical evaluation of various counts of the PRP group vs. the PPP group is shown in Fig. 2. A comparison of the H12–PEG–polyAlb group vs. the PEG-polyAlb or the saline group as shown in Fig. 3 was also carried out using Tukey–Kramer tests. A P value of less than 0·05 was considered to be statistically significant. Statistical analyses were performed using StatView software (HULINKS Inc., Tokyo, Japan).

RESULTS

Characterization of H12–PEG–polyAlb

We modified the surface of polyAlb particles (diameter of 240 ± 100 nm) with MALPEG and mPEG, and the number of MALPEG and mPEG molecules that chemically bound to one polyAlb particle was estimated to be approximately $1{\cdot}2 \times 10^4$ and $6{\cdot}1 \times 10^4$ molecules, respectively, by the indirect quantification of free PEG molecules. Furthermore, the number of H12 conjugated per polyAlb was estimated to be approximately $1{\cdot}0 \times 10^4$. The endotoxin concentration in the suspension of H12–PEG–polyAlb at an rHSA concentration of 10 mg mL^{-1} was below 0·25 EU mL^{-1}, and this was acceptable for the *in vivo* study.

Busulphan-induced thrombocytopenic rabbits

Rabbits that received busulphan at total doses of 40 and 50 mg kg^{-1} developed profound thrombocytopenia with a decline in platelet count to the half-maximal value on day 7, and the count reached the lowest value on days 15 and 14, respectively (Fig. 1). However, the haematocrit and leucocytes of these rabbits also decreased, and the rabbits became anaemic and purpuric as shown in Table 1. On the other hand, at a total dose of 30 mg kg^{-1}, thrombocytopenia was just as profound as at the higher doses of busulphan, and the rabbits showed a decline in platelet count to the half-maximal value on day 7. On days 13, 14 and 15, the platelet counts were $6{\cdot}9 \pm 0{\cdot}1$, $3{\cdot}5 \pm 1{\cdot}0$ and $2{\cdot}4 \pm 1{\cdot}3 \times 10^4$ per microlitre, respectively, which were equivalent to 1/15 or 1/20 of the platelet counts of normal rabbits ($37{\cdot}3 \pm 7{\cdot}6 \times 10^4$ per microlitre). There was a slight decrease in the leucocyte counts of the busulphan-treated rabbits compared with normal rabbits, and the haematocrits were unchanged, as shown in Table 1. After the platelet counts reached their lowest point on day 15, the count persisted for at least 1 day, then gradually started to rise, and recovered to the normal level on day 20. Consequently, for the *in vivo* experiment, we used rabbits having the most severe thrombocytopenia on day 15 after the busulphan treatment to evaluate the haemostatic ability of H12–PEG–polyAlb.

Platelet transfusion and measurement of ear bleeding time

When the PRP with counts of $0{\cdot}4 \times 10^9$, $1{\cdot}2 \times 10^9$, $2{\cdot}0 \times 10^9$ and $4{\cdot}0 \times 10^9$ per kilogram ($1{\cdot}0 \times 10^5$,

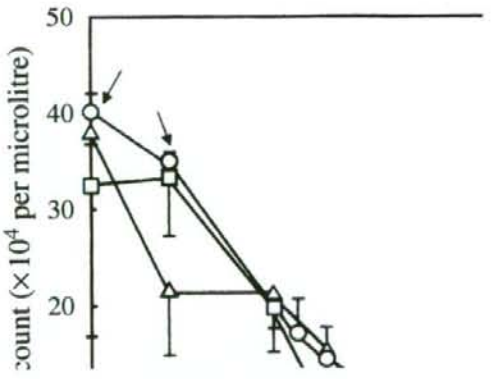

Fig. 1. Dose–response effect of busulphan on rabbits. Rabbits were treated with busulphan at a total dose of 30 mg kg^{-1} (○), 40 mg kg^{-1} (△) or 50 mg kg^{-1} (□). Ear vein blood was collected at defined intervals and platelet counts were measured. Arrows indicate the injection day of busulphan (n = 3).

Table 1. Haematological parameters on day 15 after busulphan injection

	Haematocrit (%)	White blood cell ($\times 10^3$ per microlitre)	Platelet ($\times 10^4$ per microlitre)
Normal	33·5 ± 4·2	3·1 ± 1·2	37·3 ± 7·6
Busulphan 30 mg kg^{-1}	31·3 ± 2·1	3·0 ± 1·8	2·4 ± 1·3
Busulphan 40 mg kg^{-1}	27·7 ± 4·0	2·7 ± 1·0	0·4 ± 0·1
Busulphan 50 mg kg^{-1}	26·6 ± 3·1	1·7 ± 1·5	1·0 ± 0·3

$3{\cdot}0 \times 10^5$, $5{\cdot}0 \times 10^5$, and $1{\cdot}0 \times 10^6$ per microlitre at a dose of 4 mL kg^{-1}, respectively) was transfused intravenously into the thrombocytopenic rabbits (platelet = $2{\cdot}1 \pm 0{\cdot}5 \times 10^4$ per microlitre), the platelet counts gradually increased with time, reaching maximal values 30 min after transfusion, which were $2{\cdot}2 \pm 1{\cdot}1$, $3{\cdot}2 \pm 0{\cdot}9$, $4{\cdot}0 \pm 1{\cdot}1$ and $6{\cdot}1 \pm 0{\cdot}8 \times 10^4$ per microlitre, respectively (Fig. 2). The mean percentages of recovery at 30 min after transfusion were calculated to be 65·1 ± 14·8, 65·4 ± 22·1, 66·7 ± 15·8 and 76·6 ± 9·2%, respectively. Furthermore, the half-life and survival time of transfused platelets at a dose of $2{\cdot}0 \times 10^9$ per kilogram were estimated to be 39·1 ± 6·1 and 56·4 ± 5·5 h, respectively. However, the platelet count did not change before and after PPP transfusion.

The ear bleeding times of the normal rabbits (platelet = $37{\cdot}3 \pm 7{\cdot}6 \times 10^4$ per microlitre) and the thrombocytopenic rabbits (platelet = $2{\cdot}4 \pm 1{\cdot}3 \times 10^4$ per microlitre) after the saline injection were 112 ± 24 and 1695 ± 197 s, respectively (Fig. 3). The bleeding time of the thrombocytopenic rabbits was approximately 15 times longer than that of the normal rabbits. The bleeding time at 30 min after PPP transfusion was 1473 ± 442 s, which was almost comparable to that obtained with the control thrombocytopenic rabbits injected with saline. At doses of $0{\cdot}4 \times 10^9$, $1{\cdot}2 \times 10^9$, $2{\cdot}0 \times 10^9$ and $4{\cdot}0 \times 10^9$ per kilogram, there was a dose-dependent reduction in the bleeding time of the PRP, and the bleeding time was significantly reduced to 1505 ± 410, 863 ± 540, 867 ± 440 and 505 ± 257 s, respectively (Fig. 2).

Haemostatic effects of the H12–PEG–polyAlb

When the H12–PEG–polyAlb at the dose of 40 mg kg^{-1} was injected into the thrombocytopenic rabbits, the bleeding time was not reduced (1416 ± 533 s) and was comparable to the that of control PEG-polyAlb at a dose of 40 mg kg^{-1} (1431 ± 402 s), as shown in Fig. 3. However, intravenous administration of the H12–PEG–polyAlb at a dose of 80 mg kg^{-1} significantly reduced the bleeding time to 834 ± 266 s compared with administration of saline (1695 ± 197 s) or the control PEG–polyAlb (1592 ± 286 s) at a dose of 80 mg kg^{-1}. At a dose of 120 mg kg^{-1}, the H12–PEG–polyAlb also significantly reduced the bleeding time to

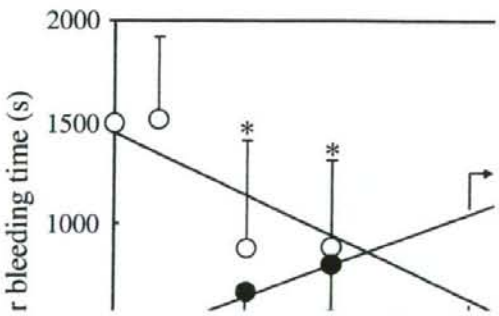

Fig. 2. Effects of platelet transfusion on ear bleeding time (○). The transfused amounts of platelets were $0{\cdot}4 \times 10^9$, $1{\cdot}2 \times 10^9$, $2{\cdot}0 \times 10^9$ and $4{\cdot}0 \times 10^9$ per kilogram. Platelet count in the rabbits at 30 min after platelet transfusion (●) ($n = 6$).
*$P < 0{\cdot}05$ vs. PPP group.

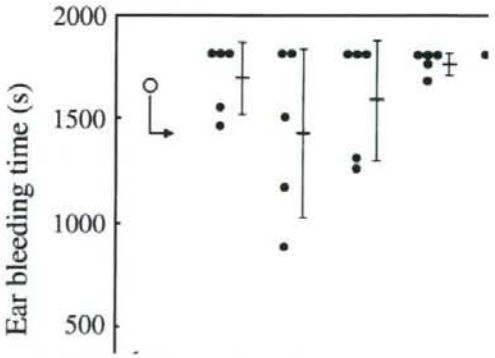

Fig. 3. Haemostatic effects of the H12–PEG–polyAlb on ear bleeding time (●). The administered amount of H12–PEG–polyAlb was 40, 80 and 120 mg kg^{-1} equivalent of rHSA. (○)indicates platelet count in the rabbits ($n = 5$–6).
*$P < 0{\cdot}05$ vs. saline group, and †$P < 0{\cdot}05$ vs. PEG–polyAlb group at the same dose.

990 ± 294 s compared with the control PEG–polyAlb (1772 ± 49 s), and the reduction effect was comparable to the response to the H12–PEG–polyAlb at a dose of 80 mg kg^{-1}.

Measurement of blood coagulation parameters

Three blood coagulation parameters, PT, APTT and Fbg, were evaluated for the rabbit blood approximately 60 min after the measurement of bleeding time, as listed in Table 2. No significant difference was seen between the sample groups (H12–PEG–polyAlb and PEG–polyAlb) and the control saline group, indicating no influence of the H12–PEG–polyAlb particles on the endogenous and exogenous coagulation activities.

DISCUSSION

We previously succeeded in prolonging the *in vivo* blood residence time of H12-conjugated polyAlb by PEG modification (H12–PEG–polyAlb), and we confirmed that the H12–PEG–polyAlb maintained an ability to specifically bind activated platelets (Okamura *et al.*, 2007). Furthermore, the H12–PEG–polyAlb dose dependently shortened the tail bleeding time of rats with moderate thrombocytopenia (Okamura *et al.*, 2007). In this study, we have evaluated the haemostatic effects of H12–PEG–polyAlb as a platelet substitute using larger animals with severe thrombocytopenia (thrombocytopenic rabbits).

We conjugated H12 to the surface of polyAlb particles modified with PEG chains, estimating the conjugation density on the polyAlb surface as approximately $4{\cdot}6 \times 10^4$ molecules μm^{-2}. We previously confirmed that the conjugation density of H12 over $4{\cdot}6 \times 10^4$ molecules μm^{-2} needs to maintain binding ability towards activated platelets, based on the flow cytometric analyses (Okamura *et al.*, 2005b, 2007). The density was similar to that of the H12–PEG–polyAlb in our previous studies, which enhanced thrombus formation under the *in vitro* flow conditions and significantly reduced the tail bleeding time of thrombocytopenic rats. However, the number of GPIIb/IIIa on one platelet is approximately $8{\cdot}0 \times 10^4$ molecules, of which density is calculated to be approximately $4{\cdot}1 \times 10^3$ molecules μm^{-2} based on the diameter of typical platelet (approximately 2·5 μm), referring to a report by Wagner *et al.* (1996). Consequently, the conjugation number of H12 on the surface of the polyAlb particle was 10-fold level in comparison with that of GPIIb/IIIa.

Next, we induced severe thrombocytopenia in the rabbits using busulphan in order to evaluate the haemostatic ability of the H12–PEG–polyAlb *in vivo*. We obtained a platelet extinction curve similar to that seen in previous studies (Kuter & Rosenberg, 1995). Sola *et al.* (2001) previously reported that a low haematocrit resulted in a significant prolongation in the bleeding time. In fact, the bleeding times on day 15 of all rabbits that received busulphan at total doses of 40 or 50 mg kg^{-1} were not measurable because the bleeding did not stop for more than 30 min (data not shown). From the haematological indices data in shown in Table 1, we evaluated conditions producing a low platelet count but maintaining a constant haematocrit value, and we determined that the appropriate busulphan dose was 30 mg kg^{-1} for the rabbits. Furthermore, the bleeding time of the thrombocytopenic rabbits on day 15 was significantly extended in comparison with that of the normal rabbits and the thrombocytopenic rabbits on day 13 or 14 (data not shown). We decided that the ear incision was to be made on day 15 and prepared the severely thrombocytopenic rabbits.

We judged that there are specific haemostatic effects when H12–PEG–polyAlb was significantly reduced the ear bleeding time of thrombocytopenic rabbits in comparison with saline and control PEG–polyAlb (H12 non-conjugation) groups. Using these rabbits, we confirmed the significant haemostatic effect of the H12–PEG–polyAlb at the doses of 80 and 120 mg kg^{-1}, although a dose-dependent reduction was not observed, as shown in Fig. 3. However, the H12–PEG–polyAlb at a dose of 40 mg kg^{-1} did not produce this effect. We previously reported a significant haemostatic effect of H12–PEG–polyAlb at a dose of 40 mg kg^{-1} using rats with moderate thrombocytopenia (Okamura *et al.*, 2007). The present results indicate that a higher dose of the H12–PEG–polyAlb was necessary to assist platelet haemostasis in the

Table 2. Blood coagulation parameters after administration of H12–PEG–polyAlb at a dose of 80 mg kg^{-1}

	PT (s)	APTT (s)	Fbg (g dL^{-1})
Saline (normal)	8·1 ± 0·2	26·1 ± 1·2	256·6 ± 15·3
Saline (thrombocytopenia)	8·3 ± 0·6	23·6 ± 5·3	259·7 ± 15·2
PEG–polyAlb	8·5 ± 0·5	26·1 ± 2·0	264·2 ± 26·6
H12–PEG–polyAlb	8·4 ± 0·4	24·7 ± 3·8	267·8 ± 10·3

severe thrombocytopenia model. Based on our previous studies of the H12 particles under flow conditions *in vitro* (Takeoka *et al.*, 2003), we hypothesized that the H12–PEG–polyAlb would work at the vascular injury by the following mechanisms: (1) adhesion of the H12–PEG–polyAlb could be initiated by the activated platelets, which had already adhered on the surface of the exposed collagen at the vascular injury, (2) the H12–PEG–polyAlb adhering to the surface of the platelet could provide additional binding sites for activated platelets and (3) the H12–PEG–polyAlb could accelerate thrombus formation by enhancing aggregation of the flowing platelets. However, in the case of severe thrombocytopenia, adhesion of the H12–PEG–polyAlb decreased because the fewer platelets adhered on the collagen. It was suggested that higher doses of the H12–PEG–polyAlb would be necessary to assist platelet haemostasis by recruiting the flowing platelets and filling up the vascular injury site using the volume of the H12–PEG–polyAlb particles. However, considering the dose-independent reduction of the particles, it was also suggested that there was a limited time window for the H12–PEG–polyAlb to accumulate and fill up the vascular injury site and that additional processes such as amplification of platelet aggregation and blood coagulation would be necessary to further promote platelet haemostasis.

Furthermore, we also confirmed that haematological indices (data not shown) and coagulation parameters as shown in Table 2 did not change before and after the infusion of the H12–PEG–polyAlb, suggesting that the polyAlb was a safe particle with a minimal likelihood of causing side effects after injection.

We used a platelet transfusion model as a positive control for the platelet substitutes. The survival time of the transfused platelets was comparable to that obtained from the ^{51}Cr and ^{111}In-labelled platelets evaluated in previous reports (Packham *et al.*, 1992; Franco *et al.*, 1994), whereas the mean percentage of recovery was similar to the that in previous reports (Packham *et al.*, 1992; Franco *et al.*, 1994; Rand *et al.*, 2002). Furthermore, confirmation of a dose-dependent reduction in the bleeding time after administering PRP to severe thrombocytopenic rabbits established a positive control for comparison with platelet substitutes. We proposed the following equation (Eqn 1) relating the transfused platelet counts to the bleeding time as follows:

$$y = -252{\cdot}03x + 1425{\cdot}6 (r^2 = 0{\cdot}85) \qquad (1)$$

where the x value gives the PRP (10^9 per kilogram) and y value gives the ear bleeding time (s). We estimated the haemostatic capacity of H12–PEG–polyAlb using Eqn 1. The bleeding time (834 ± 266 s) of the H12–PEG–polyAlb at a dose of 80 mg kg^{-1} (approximately $7{\cdot}4 \times 10^{13}$ particles kg^{-1}) was similar to that following platelet transfusion at a dose of $2{\cdot}4 \times 10^9$ per kilogram. Similarly, in the case of 120 mg kg^{-1} (approximately $1{\cdot}1 \times 10^{14}$ particles kg^{-1}), the bleeding time of the H12–PEG–polyAlb was similar to that of platelet transfusion at a dose of $1{\cdot}7 \times 10^9$ per kilogram. These results indicate the haemostatic capacity of the H12–PEG–polyAlb at the particle number $3{\cdot}1 \times 10^4$ to $6{\cdot}5 \times 10^4$ would correspond to that of one platelet. We also evaluated the haemostatic capacity based on the total injected particle volume because the particle diameter of the H12–PEG–polyAlb (240 ± 100 nm) is 10-fold smaller than that of a typical platelet (2–3 μm). We calculated that the volume of the particles required for haemostatic support was 31- to 65-fold less than that of platelets that would produce a similar effect.

In conclusion, the H12–PEG–polyAlb significantly shortened the ear bleeding time of severely thrombocytopenic rabbits. We assessed the haemostatic capacity of the H12–PEG–polyAlb based on comparisons with platelet transfusions and calculated that the haemostatic capacity of the H12–PEG–polyAlb was approximately 31- or 65-fold greater than that of a similar volume of platelets. Thus, the H12–PEG–polyAlb may be a suitable candidate for an alternative to human platelet concentrates infused to treat bleeding in patients with severe thrombocytopenia. In future, we plan to assess the haemostatic ability of the H12–PEG–polyAlb to treat animals with severe thrombocytopenia resulting from blood loss during surgery.

ACKNOWLEDGMENTS

The authors thank M. Murata, MD, PhD, and K. Yokoyama, MD, PhD, at Keio University for useful discussion about the functional evaluation of H12 peptide and blood coagulation parameters. This work was supported in part by Health and Labor Sciences Research Grants (Research on Pharmaceutical and Medical Safety, S. T., Y. I. and M. H.), Ministry of Health, Labor and Welfare, Japan. Y. O. was the recipient of Japan Health Sciences Foundation. T. F. was the scholar 'Doctor-21' of Yoshida Scholarship Foundation.

REFERENCES

Agam, G. & Livine, A.A. (1992) Erythrocytes with covalently bound fibrinogen as a cellular replacement for

the treatment of thrombocytopenia. *European Journal of Clinical Investigation*, **22,** 105–112.

Casals, E., Verdaguer, A., Tonda, R., Galan, A., Escolar, G. & Estelrich, J. (2003) Atomic force microscopy of liposomes bearing fibrinogen. *Bioconjugate Chemistry*, **14,** 593–600.

Coller, B.S., Springer, K.T., Beer, J.H., Mohandas, N., Scudder, L.E., Norton, K.J. & West, S.M. (1992) Thromboerythrocytes. In vitro studies of a potential autologous, semi-artificial alternative to platelet transfusion. *Journal of Clinical Investigation*, **89,** 546–555.

De Marco, L., Girolami, A. & Zimmerman, T.S. (1986) Von Willebrand factor interaction with the glycoprotein IIb/IIIa complex. *Journal of Clinical Investigation*, **77,** 1272–1277.

Franco, R.S., Lee, K.N., Barker-Gear, R., Gates, R. & Menitove, J.E. (1994) Use of bi-label biotinylation for concurrent measurement of in vivo recovery and survival in two rabbit platelet populations. *Transfusion*, **34,** 784–789.

Graham, S.S., Gonchoroff, N.J. & Miller, J.L. (2001) Infusible platelet membranes retain partial functionality of the platelet GPIb/IX/V receptor complex. *American Journal of Clinical Pathology*, **115,** 144–147.

Kitaguchi, T., Murata, M., Iijima, K., Kamide, K., Imagawa, T. & Ikeda, Y. (1999) Characterization of liposomes carrying von Willebrand factor-binding domain of platelet glycoprotein Ibα: a potential substitute for platelet transfusion. *Biochemical and Biophysical Research Communications*, **261,** 784–789.

Kloczewiak, M., Timmons, S. & Hawiger, J. (1982) Localization of a site interacting with human platelet receptor on carboxy-terminal segment of human fibrinogen γ chain. *Biochemical and Biophysical Research Communications*, **107,** 181–187.

Kloczewiak, M., Timmons, S., Lukas, T.J. & Hawiger, J. (1984) Platelet receptor recognition site on human fibrinogen. Synthesis and structure-function relationship of peptides corresponding to the carboxy-terminal segment of the γ chain. *Biochemistry*, **23,** 1767–1774.

Kloczewiak, M., Timmons, S., Bednarek, M.A., Sakon, M. & Hawiger, J. (1989) Platelet receptor recognition domain on the γ chain of human fibrinogen and its synthetic peptide analogues. *Biochemistry*, **28,** 2915–2919.

Kuter, D.J. & Rosenberg, R.D. (1995) The reciprocal relationship of thrombopoietin (c-Mpl ligand) to changes in the platelet mass during busulfan-induced thrombocytopenia in the rabbit. *Blood*, **85,** 2720–2730.

Lam, S.C., Plow, E.F., Smith, M.A., Andrieux, A., Ryckwaert, J.J., Marguerie, G. & Ginsberg, M.H. (1987) Evidence that arginyl-glycyl-aspartate peptides and γ chain peptides share a common binding site on platelets. *Journal of Biological Chemistry*, **262,** 110–115.

Levi, M., Friedrich, P.W., Middleton, S. *et al.* (1999) Fibrinogen-coated albumin microcapsules reduce bleeding in severely thrombocytopenic rabbits. *Nature Medicine*, **5,** 107–111.

Michelson, A.D., Barnard, M.R., Hechtman, H.B., MacGregor, H., Connolly, R.J., Loscalzo, J. & Valeri, C.R. (1996) In vivo tracking of platelets: circulating degranulated platelets rapidly lose surface P-selectin but continue to circulate and function. *Proceedings of National Academy of Sciences of the United State of America*, **93,** 11877–11882.

Mustard, J.F., Packham, M.A. & Kinlough-Rathbone, R.L. (1978) Fibrinogen and ADP-induced platelet aggregation. *Blood*, **52,** 453–466.

Nishiya, T., Kainoh, M., Murata, M., Handa, M. & Ikeda, Y. (2002) Reconstitution of adhesive properties of human platelets in liposomes carrying both recombinant glycoproteins Ia/IIa and Ibα under flow conditions: specific synergy of receptor-ligand interactions. *Blood*, **100,** 136–142.

Okamura, Y., Maekawa, Y., Teramura, Y., Maruyama, H., Handa, H., Ikeda, Y. & Takeoka, S. (2005a) Hemostatic effects of phospholipid vesicles carrying fibrinogen-γ chain dodecapeptide in vitro and in vivo. *Bioconjugate Chemistry*, **16,** 1589–1596.

Okamura, Y., Takeoka, S., Teramura, Y., Maruyama, H., Tsuchida, E., Handa, M. & Ikeda, Y. (2005b) Hemostatic effects of fibrinogen γ-chain dodecapeptide-conjugated polymerized albumin particles in vitro and in vivo. *Transfusion*, **45,** 1221–1228.

Okamura, Y., Fujie, T., Maruyama, H., Handa, M., Ikeda, Y. & Takeoka, S. (2007) Prolonged hemostatic ability of poly(ethylene glycol)-modified polymerized albumin particles carrying fibrinogen γ-chain dodecapeptide. *Transfusion*, **47,** 1254–1262.

Packham, M.A., Rand, M.L. & Kinlough-Rathbone, R.L. (1992) Similarities and differences between rabbit and human platelet characteristics and functions. *Comparative Biochemistry and Physiology A*, **103,** 35–54.

Rand, M.L., Wang, H., Mody, M., Chu, I., Treutiger, I., Nguyen, A., Packham, M.A. & Freedman, J. (2002) Concurrent measurement of the survival of two populations of rabbit platelets labeled with either two PKH lipophilic dyes or two concentrations of biotin. *Cytometry*, **47,** 111–117.

Reimers, H.J., Buchanan, M.R. & Mustard, J.F. (1973) Survival of washed rabbit platelets in vivo. *Proceedings of the Society for Experimental Biology and Medicine*, **142,** 1222–1225.

Ruggeri, Z.M., De Marco, L. & Gatti, L. (1983) Platelets have more than one binding site for von Willebrand factor. *Journal of Clinical Investigation*, **72,** 1–12.

Rybak, M. & Renzulli, L.A. (1993) A liposome based platelet substitutes, the plateletsome, with hemostatic efficacy. *Biomaterials, Artificial Cells, and Immobilization Biotechnology*, **21,** 108–118.

Sola, M.C., del Vecchio, A., Edwards, T.J., Suttner, D., Huston, A.D. & Christensen, R.D. (2001) The relationship between hematocrit and bleeding time in very low birth weight infants during the first week of life. *Journal of Perinatology*, **21,** 368–371.

Takagi, J., Petre, B.M., Walz, T. & Springer, T.A. (2002) Global conformational rearrangements in integrin extracellular domains in outside-in and inside-out signaling. *Cell*, **110,** 599–611.

Takeoka, S., Teramura, Y., Ohkawa, H., Ikeda, Y. & Tsuchida, E. (2000) Conjugation of von Willebrand factor-binding domain of platelet glycoprotein Ibα to size-controlled albumin microspheres. *Biomacromolecules*, **1,** 290–295.

Takeoka, S., Teramura, Y., Okamura, Y., Handa, M., Ikeda, Y. & Tsuchida, E. (2001) Fibrinogen-conjugated albumin polymers and their interaction with platelets under flow conditions. *Biomacromolecules*, **2,** 1192–1197.

Takeoka, S., Teramura, Y., Okamura, Y., Tsuchida, E., Handa, M. & Ikeda, Y. (2002) Rolling properties of rGPIbα-conjugated phospholipid vesicles with different membrane flexibilities on vWf surface under flow conditions. *Biochemical and Biophysical Research Communications*, **296,** 765–770.

Takeoka, S., Okamura, Y., Teramura, Y., Watanabe, N., Suziki, H., Tsuchida, E., Handa, M. & Ikeda, Y. (2003) Function of fibrinogen γ-chain dodecapeptide-conjugated latex beads under flow. *Biochemical and Biophysical Research Communications*, **312,** 773–779.

Teramura, Y., Okamura, Y., Takeoka, S. *et al.* (2003) Hemostatic effects of polymerized albumin particles bearing rGPIa/IIa in thrombocytopenic mice. *Biochemical and Biophysical Research Communications*, **306,** 256–260.

The Panel on Diagnostic Application of Radioisotopes in Hematology, International Committee for Standardization in Hematology. Recommended methods for radioisotope platelet survival studies. (1977) *Blood*, **50,** 1137–1144.

Wagner, C.L., Mascelli, M.A., Neblock, D.S., Weisman, H.F., Coller, B.S. & Jordan, R.E. (1996) Analysis of GPIIb/IIIa receptor number by quantification of 7E3 binding to human platelets. *Blood*, **88,** 907–914.

Wertheimer, E., Shapiro, B. & Fodor-Salomonowicz, I. (1944) Stability of fibrinogen in normal and pathological plasma. *British Journal of Experimental Pathology*, **25,** 121–125.

Xiao, T., Takagi, J., Coller, B.S., Wang, J.H. & Springer, T.A. (2004) Structural basis for allostery in integrins and binding to fibrinogen-mimetic therapeutics. *Nature*, **432,** 59–67.

血栓止血誌 19(6) : 774~778, 2008

◆特集：血小板を作ろう　総説◆

血小板代替物

半田　誠[*1]，岡村陽介[*2]，武岡真司[*2]，
池田康夫[*3]

半田　誠

1976年3月　慶應義塾大学医学部卒業
1980年7月　慶應義塾大学助手（血液内科学）
1991年4月　慶應義塾大学専任講師（輸血センター室長）
2000年4月　慶應義塾大学助教授（輸血センター室長）
2007年4月　慶應義塾大学准教授（輸血・細胞療法部長）

Platelet substitutes

Makoto HANDA[*1], Yosuke OKAMURA[*2], Shinji TAKEOKA[*2], Yasuo IKEDA[*3]

Key words: Platelet substitute, Platelet transfusion, Fibrinogen-coated albumin particles, H12-coated liposomes, ADP encapsulation

はじめに

血小板は一次血栓形成を通じて生体の止血機構の中心をなし，その量的・質的異常により惹起される出血の予防や治療に対し唯一信頼できる手段は血小板輸血である．高度な医療に必須な血小板の必要量は将来も減少することはなく，一方，人口減と高齢化に伴う献血者数の低下などでその供給量の減少が予想されること，そして，短い期限（4日）で厳密な保存条件が要求されることから災害時等への緊急対応が極めて困難であること，などから液状の血小板濃厚液に代わる安定的な製造物（血小板代替物，platelet substitutes）の開発が行われてきた．

血小板代替物の種類（図1）

広義の血小板代替物は，血小板そのものを加工した血小板由来産物と，血小板以外の構成成分から成り立った人工産物に大別され，後者がいわゆる狭義の血小板代替物（人工血小板：artificial platelets）である[1]．前者の開発の歴史は古く，米国において軍事目的のための国防費による研究が実に50年代から始まった．その結果，固定血小板や凍結乾燥血小板，あるいは凍結乾燥した血小板膜断片（infusible platelet membrane：IPM）などが開発され，IPMは初期臨床研究（フェーズI/II）に供された．一方，後者は生体適合性のある担体（赤血球，アルブミン微粒子，リン脂質小胞体：リポソームなど）を用い，その表面に血小板受容体やリガンドを結合させたもので，90年代初めにフィブリノゲンやその合成ペプチド（RGD）をコートした赤血球（Thromboerythrocyte）が先駆けとなり，いくつかの微粒子が開発され，フィブリノゲンを表面固定したアルブミン微粒子（Synthocyte™

[*1]慶應義塾大学輸血・細胞療法部〔〒160-8582 新宿区信濃町35〕
Department of Transfusion Medicine & Cell Therapy, School of Medicine, Keio University
〔35 Shinanomachi, Shinjuku, Tokyo 160-8582, Japan〕
Tel: 03-3353-1211 (ext. 62123)　Fax: 03-3353-9706　e-mail: mhanda@sc.itc.keio.ac.jp
[*2]早稲田大学理工学術院
Department of Life Science and Medical Bioscience, Graduate School of Advanced Science and Engineering, Waseda University
[*3]慶應義塾大学内科
Department of Internal Medicine, School of Medicine, Keio University

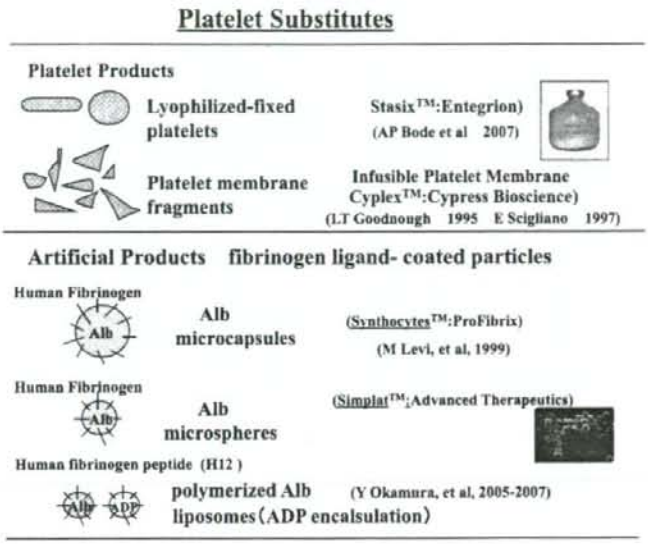

図1　開発された血小板代替物

やSimplat™）は初期臨床研究に供された．

血小板代替物の開発戦略

血小板代替物が具備可能な血小板機能は，#1：止血局所への特異的な集積能力，#2：血小板血栓（血小板凝集）を促進する能力，#3：フィブリン血栓の形成促進能力すなわち凝固活性，であると考えられる．実際，血小板輸血が必要な場合にも患者の血小板が全くなくなることはない．生きた血小板と同等の機能を人工的に創出することは事実上不可能であり，残存した患者血小板を有効に止血局所で働かせるような機能を最小限保有した製造物が合理的かつ実際的である．一方，安全性の面で重要なのは，その機能は止血局所でのみ特異的に働き，全身的な血栓形成を促すものではけっしてないことである．また，適応に関しての重要なポイントは，出血の予防までを目的とするのか，あるいは単に緊急避難的な止血効果を狙った治療薬とするのかである．出血予防を目的とする場合は，血中での滞留時間をできるだけ長く保つ必要があり，生体適合性を高める目的で，粒子径を可及的に小さくしたり，あるいはポリエチレングリコール鎖による表面修飾（PEG化）を行ったりする工夫が必要である．一方，緊急時の止血薬として使用するならば，血中滞留時間は短くても問題はない．

血小板代替物：各論

前臨床を経て，実際にヒトへの臨床試験まで行き着いたものは数えるほどしかなく，しかも未だにどれも実用化には至っていない．また，そのほとんどがベンチャー企業主導のもとで開発されたもので，したがってそのデータの詳細はほとんど公表されていない．

1）血小板由来産物

凍結乾燥血小板膜断片（IPM：Cyplex™）と

50年近くの試行錯誤の結果開発された固定凍結乾燥血小板（Stasix™）が双璧である[2)3)]．両者ともその表面のGPIb/IX受容体はインタクトで，それ介したフォンビレブランド因子（VWF）との結合により，止血局所への特異的集積性を有する．また，特徴として，止血局所でその表面を介した凝固因子活性化によるトロンビン生成を助長する働きがある．一方，フィブリノゲノなどと結合して血小板凝集を活性化依存性に惹起するのがGPIIb/IIIa受容体であるが，これらの産物では当然のことながら活性化機構は損なわれており，血小板凝集は起こさない．特にIPMは他に先駆けて臨床試験を行い，フェーズII試験では，5万以下の血小板減少症患者40例のうち27例（65%）で出血症状の改善をきたした[1)]．しかし，その後のフェーズIII試験の後，その理由は公表されないまま開発は中止された．一方，後者は，現在も開発が続けられており，マイルドな条件下でのアルデヒド固定により，血小板の細胞内のシグナル伝達機構の一部は保存され，したがってその表面のGPIb/IX受容体と止血部位に発現したVWFを介した局所集積性を示した後の活性化ステップにより，膜表面の変化を来たして，凝固因子カスケード促進の場を提供すること（凝固活性）で，強力な止血作用を及ぼすとされている[2)]．Stasix™の血中停留時間は極めて短く（半減期：10分），したがって全身性の血栓惹起作用は避けることができるとされ，緊急避難的な（たとえば戦場）止血治療薬として開発が進められている．

2）人工血小板代替物

初期には赤血球が用いられたが，その後は生体適合性に優れたアルブミンとリポソームの2種類が担体（微粒子）として，また認識表面としてヒトフィブリノゲンやその関連ペプチド（RGDなど）などのリガンドを用いたものが主流である[1)]．一方，遺伝子組み換えの血小板接着受容体（GPIbα断片，コラーゲン受容体のGPIa/IIa受容体断片）を認識表面とした人工物もいくつか発表されたが，実用化の面から人工血小板としての検討はそれ以上なされていない[4)]．

（1）アルブミン微粒子

フィブリノゲンやそのRGDペプチドが表面固定された赤血球（Thromboerythrocyteなど）は，フィブリノゲンの受容体であるGPIIb/IIIa複合体を介して活性化血小板と特異的に結合することで血小板凝集を促進して，止血効果を来すことが明らかとなり，赤血球の代わりにアルブミン微粒子を用いたフィブリノゲン結合人工物がいくつか開発された[1)5)]．1995年には，平均径が1.2ミクロンのアルブミン・マイクロスフェアー（Simplat™）が，1999年には，より大型の平均径3.5～4.5ミクロンのアルブミン・マイクロカプセル（Synthocyte™）が報告され，前者はフェーズIII，後者は少なくともフェーズIIまでの臨床試験が行われた[1)6)]．いずれも血液疾患に伴う血小板減少症患者の出血の治療と予防に適用されたが，その結果は公表されておらず，いまだ実用化されていない．2003年には，厚生労働科学研究費の補助により我が国で開発されたアルブミン重合体が報告された．この人工物は認識表面としフィブリノゲンのGPIIb/IIIa複合体に特異的な結合部位であるγ鎖C末端ドデカ配列由来合成ペプチド（^{400}HHLGGAKQAGDV^{411}：H12）を担持させることで，その活性化血小板への特異性を増した．またそのサイズは，0.2ミクロンとより小型で，表面をPEG化することで，その血中滞留時間（半減期：約8時間）を大幅に延ばすことに成功した[7)]．一方，アルブミン・マイクロスフェアーの表面にフィブリノゲンそのものではなくヒトフィブリノゲン親和性合成ペプチドを担持させた人工物（HaemoPlax™）が開発された（http://www.haemostatix.com/）．これは，投与後，血中のフィブリノゲンが表面にコートされて止血効果を来すとされている．いずれの微粒子もその止血作用は，活性化血小板に結合して血小板凝集を増強することで発揮されると考えられ

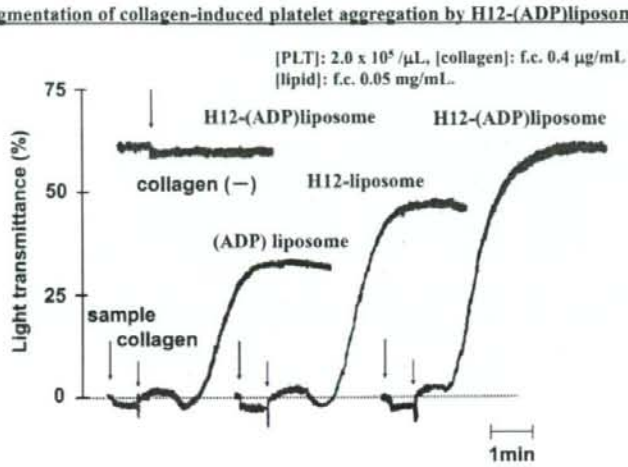

図2　H12結合リポソームのコラーゲン惹起血小板凝集増強作用(ADP内包化の効果)[8]

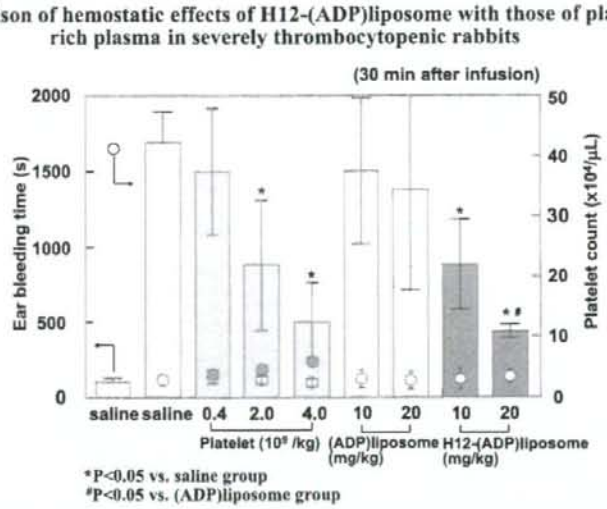

図3　H12結合（ADP）リポソームのウサギ血小板減少症モデルにおける出血時間短縮効果（血小板輸血との比較）[8]

る．したがって，その効果は残存血小板に依存することとなり，血小板数の極めて低い場合にはその止血作用は期待できない可能性がある．

(2) リポソーム

リポソームは生体適合性に優れ，すでに医薬品のDDS担体として実用に供されており，リ

ポソームを担体とした人工血小板代替物がH12結合アルブミン重合体とともに厚生労働科学研究費の補助により開発が進められてきた．実際，H12結合リポソームは *in vitro* でアゴニスト惹起血小板凝集を増強する効果が見られ，プスルファンによるラット血小板減少症モデルにおいて延長した出血時間を短縮する効果が認められた．しかし，H12結合アルブミン重合体と比較するとその効果は弱かった．これは多分，アルブミン重合体で予想される局所充填効果がリポソームでは期待できないためかもしれない．そこで，リポソームのDDS機能を用い，生理的な血小板アゴニストであるアデノシン2リン酸（ADP）を内包化したところ（H12-(ADP) リポソーム），より強力な *in vitro*（アゴニスト惹起血小板凝集増強作用），*in vivo*（血小板減少症動物モデルでの出血時間短縮作用）機能を付加することに成功した[8]（**図2, 3**）．H12-(ADP) リポソームは止血局所に特異的に集積すること，内包化したADPの放出は血小板凝集に依存していること，したがって動物モデルでは明らかな血小板の活性化や凝固系の亢進は全身的には認められなかった．ウサギ血小板減少症モデルでは，血小板輸血に匹敵した効果的な出血時間短縮効果が認められ，完全な人工物として開発の進展が期待されている．

おわりに

血小板代替物の開発の歴史は古いにもかかわらず未だに実用化に至っていない．前臨床では明らかな血小板代替機能が認められても，実際の臨床試験をクリアーできていない．しかし，開発は続けられており，その方向性は，米国での軍事目的（緊急避難的な止血薬）での凍結乾燥固定血小板，そして，一般の医療における出血の予防や治療を目的とした人工血小板微粒子（アルブミン，リポソーム）であり，いずれも臨床試験を想定した段階にあると思われる．

謝辞：本総説で紹介した研究の一部は平成20年度厚生労働科学研究費助成，政策創薬総合研究分野「臨床応用可能な人工血小板としてのH12結合微粒子の *in vivo* 評価」（H18-創薬-一般-026；主任研究者：半田誠）によって行われた．

文　献

1) Blajchman MA : Substitutes and alternatives to platelet transfusions in thrombocytopenic patients. J Thromb Haemost **1** : 1637-1641, 2003.
2) Graham SS, Gonchoroff NJ, Miller JL : Infusible platelet membranes retain partial functionality of the platelet GPIb/IX/V receptor complex. Am J Clin Pathol. **115** : 144-151, 2001.
3) Bode AP, Fischer TH. Lyophilized platelets : fifty years in the making. Artif Cells Blood Substit Immobil Biotechnol **35** : 125-133, 2007.
4) Nishiya T, Kainoh M, Murata M, Handa M, Ikeda Y : Reconstitution of adhesive properties of human platelets in liposomes carrying both recombinant glycoproteins Ia/IIa and Ibalpha under flow conditions : specific synergy of receptor-ligand interactions. Blood. **100** : 136-141, 2002.
5) Coller BS, Springer KT, Beer JH, Mohandas N, Scudder LE, Norton KJ, West SM : Thromboerythrocytes. In vitro studies of a potential autologous, semi-artificial alternative to platelet transfusions.J Clin Invest. **89** : 546-555, 1992.
6) Levi M, Friederich PW, Middleton S, de Groot PG, Wu YP, Harris R, Biemond BJ, Heijnen HF, Levin J, ten Cate JW : Fibrinogen-coated albumin microcapsules reduce bleeding in severely thrombocytopenic rabbits.Nat Med. **5** : 107-111, 1999.
7) Okamura Y, Fujie T, Maruyama H, Handa M, Ikeda Y, Takeoka S. Prolonged hemostatic ability of poly (ethylene glycol)-modified polymerized albumin particles carrying fibrinogen γ-chain dodecapeptide. Transfusion **47** : 1254-1262, 2007.
8) Okamura Y, Takeoka S, Eto K, Maekawa I, Fujie T, Maruyama H, Ikeda Y, Handa M : Development of fibrinogen γ-chain peptide-coated, adenosine diphosphate-encapsulated liposomes as a synthetic platelet substitute. J Thromb Haemost (in press).

Fabrication of free-standing albumin-nanosheets having heterosurfaces

Yosuke Okamura, Takahiro Goto, Daisuke Niwa, Yoshihito Fukui, Masanobu Otsuka, Norikazu Motohashi, Tetsuya Osaka, Shinji Takeoka

Consolidated Research Institute for Advanced Science and Medical Care, Waseda University, Tokyo 169-8555, Japan

Received 2 August 2007; revised 11 December 2007; accepted 11 December 2007
Published online 22 April 2008 in Wiley InterScience (www.interscience.wiley.com). DOI: 10.1002/jbm.a.31934

Abstract: Sheet-shaped carriers, having both obverse and reverse surfaces and thus a large contact area for targeting a site, have several advantages over spherical-shaped carriers, which have an extremely small contact area for targeting sites. Here, we proposed a novel method to prepare a free-standing ultrathin and biocompatible nanosheet having heterosurfaces, by a combination of four processes: (1) specific adsorption of recombinant human serum albumin (rHSA) molecules onto a patterned octadecyltrimethoxysilane self-assembled monolayer region (ODS-SAM), (2) preparation of nanosheets of rHSA molecules bearing thiol groups (SH-rHSA) via two-dimensionally disulfide crosslinking, (3) surface modification of the resulting nanosheet, and (4) preparation of the free-standing nanosheet by detachment from the ODS-SAM. The SH-rHSA molecules at pH 5.0 and a concentration of 1 μg/mL were specifically adsorbed on the patterned ODS-SAM regions by hydrophobic interaction, and were two-dimensionally crosslinked in the presence of copper ion as an oxidant. The rHSA-nanosheets were then simply detached from the ODS-SAM by treatment with surfactant. We succeeded in the preparation of rectangular (10 μm × 30 μm) and ultrathin (4.5 ± 1.0 nm) rHSA-nanosheets on a patterned ODS-SAM, and could also obtain free-standing rHSA-nanosheets having heterosurfaces by surface modification with fluorescent latex beads. Thus, the rHSA-nanosheets having heterosurfaces could be regarded as a new biomaterial for drug carriers, hemostatic reagents, wound dressing for burn injury, and so forth. © 2008 Wiley Periodicals, Inc. J Biomed Mater Res 89A: 233–241, 2009

Key words: albumin; nanosheet; free-standing; biocompatibility; crosslinking

INTRODUCTION

In recent years, much attention has been paid to drug-delivery system (DDS) as a new pharmacological approach to improve the efficacy and safety of drugs. In DDS, vesicles, micelles, emulsions, and biodegradable nanoparticles have been extensively studied as carriers for biologically active substances such as drugs, recognition proteins, enzymes, genes, and so forth.[1] There are two concepts for the development of DDS: passive and active targeting systems. In the latter case, recognition proteins such as antibodies and various ligands are conjugated to the surface of the carriers to target the tissue epitopes or specific cells.

We have developed biocompatible and biodegradable nanoparticles such as albumin-based nanoparticles[2–5] and phospholipid vesicles[6,7] carrying recombinant fragments of platelet membrane proteins[3,4,6,8] and dodecapeptide as a recognition site for fibrinogen.[2,5,7,9] These nanoparticles specifically recognized the site of bleeding injury or activated platelets. In our approach to the conjugation of high- and low-molecular-weight molecules such as glycoprotein Ibα and dodecapeptide to the surface of the particle, we observed that the activity of dodecapeptide was suppressed by the steric hindrance of the glycoprotein Ibα, and found that a spacer such as a poly(ethylene glycol) chain was needed in the conjugation of the peptides.[8]

On the other hand, sheet-shaped carriers, having both obverse and reverse surfaces and thus a large contact area for targeting a site, have several advantages over spherical-shaped carriers, which have an extremely small contact area for targeting sites. Recently, several approaches have been implemented for the fabrication of free-standing films, combining large surface area with nanoscale thickness, from polymers and/or from inorganic materials: cast films,[10] layer-by-layer assemblies of polyelectolyte multilayers,[11–15] crosslinked amphiphilic Langmuir–Blodgett films,[16] self-assembled monolayers (SAMs),[17,18] and assemblies of triblock copolymers.[19] However, there

Correspondence to: S. Takeoka; e-mail: takeoka@waseda.jp
Contract grant sponsor: Shorai Foundation for Science and Technology

have been no reports on the preparation of free-standing nanoscale sheets from biocompatible and biodegradable materials only. The nanosheets would be a candidate as a new injectable biomaterial in DDSs.

Organosilane SAMs have been widely applied to control physical and chemical properties of the surfaces of glass, quartz, SiO_2/Si wafers, or silica particles.[20] Furthermore, they are excellent tools to study the immobilization of proteins such as redox proteins,[21] enzymes,[22] and immunoglobulins, using covalent bonds or noncovalent bonds such as ionic or hydrogen bonds, van der Waals attraction, and hydrophobic interaction with the various terminal groups of SAMs. Generally, it is easy to construct patterned SAMs with uniform sizes and shapes on silicon oxide or gold substrates using conventional photolithography processes.[23] This approach was used for the electrochemical analysis of proteins immobilized by adsorption on the substrates.

Here, we proposed a novel method to prepare a free-standing biocompatible nanosheet having heterosurfaces. We used a patterned hydrophobic octadecyltrimethoxysilane-SAM (ODS-SAM) on silicon oxide to prepare nanosheets of uniform sizes and shapes. Furthermore, we modified the surface of the nanosheet with fluorescent latex beads as a model material to prove the fabrication of a nanosheet with heterosurfaces.

MATERIALS AND METHODS

Reagents

P-type Si (100) wafers (below 0.02 Ω cm) covered with thermally grown silicon oxide (~200 nm) was purchased from KST World, Co. (Fukui, Japan). *n*-Octadecyltrimethoxysilane (ODS, 97%) was purchased from Gelest (Morrisville, PA). Succinimidyl 6-[3′-(2-pyridyldithio) propionamido] hexanoate (LC-SPDP) and *N*-(ε-maleimidocaproyl) succinimide ester (EMCS) were purchased from Pierce Biotechnology (Rockford, IL). Dithiothreitol (DTT) and copper sulfate pentahydrate were purchased from Wako Pure Chemical Industries (Osaka, Japan). 5,(6)-Tetramethylrhodamine isothiocyanate (TRITC) and 7-chloro-4-nitrobenzo-2-oxa-1,3-diazole (NBD) were purchased from Invitrogen (Carlsbad, CA). Sephadex G25 for gel permeation chromatography (GPC) was purchased from GE Healthcare UK (Buckinghamshire, England). Latex beads (Polybead™, 100 nm ϕ) were purchased from Polysciences (Warrington, PA). Recombinant human serum albumin (rHSA, 250 mg/mL) was kindly donated by Oxgenix Co. (Tokyo, Japan).

SAM preparation

Silicon wafers were treated with SPM (96% H_2SO_4: 30% H_2O_2 = 4:1 (v/v)) at 120°C followed by rinsing with distilled water. The resulting wafers were placed in a 20-mL Teflon vial containing a glass cup filled with 200 μL of ODS liquid. The vials were sealed with a cap and then heated for 8 h at a constant temperature of 110°C in a dry room to prepare a hydrophobic ODS-SAM on the silicon oxide.[24]

Patterning processes

The patterned ODS-SAM having hydrophobic octadecyl regions and hydrophilic silicon oxide regions on the substrate was prepared by a conventional photolithography process. The ODS-SAM on the silicon oxide was covered with a photoresist (OFPR-800 500 cP, Tokyo Ohka Kogyo, Co., Kanagawa, Japan), and was irradiated with a 350-nm UV lamp (MA-10, Mikasa, Tokyo, Japan) using a photomask (size: 1 cm × 1 cm, patterning; rectangle (10 μm × 30 μm), Topic Co., Saitama, Japan). After developing (NMD-3), the substrate was exposed to oxygen plasma (Plasma Reactor PR301, Yamato Scientific Co., Tokyo, Japan) at an input power of 200 W and an oxygen flow rate of 80 sccm for removal of ODS. The photoresist was removed by acetone washing to obtain the patterned ODS-SAM.

Contact angle measurements

A 3-μL drop of distilled water was placed directly onto the ODS-SAM with a micropipette before and after rHSA adsorption, or after the addition of surfactant as described earlier. The liquid drops were observed with an optical microscope with 5× magnification. All water contact angles represented the mean ± SD of the five measurement values.

Chemical modification of rHSA with thiol groups

An rHSA solution (250 mg/mL) was diluted to 50 mg/mL with a phosphate buffer solution (pH 7.4). A 50 m*M* solution of LC-SPDP in DMSO (150 μL) was added to the rHSA solution (1 mL), and the solution was incubated for 20 min at r.t. To the rHSA solution, a 10 m*M* TRITC phosphate buffer solution (112.5 μL, pH 7.4) was then added and incubated for 20 min at r.t. The unreacted LC-SPDP (precipitated), TRITC, and the byproducts were separated by centrifugation, and then by GPC with an acetate buffer (pH 5.0) to obtain a pyridyl disulfide-bearing rHSA (PD-rHSA). DTT [final concentration (f.c.) 20 m*M*] was added to the PD-rHSA solution to reduce the PD group to a SH group. The unreacted DTT and the byproducts were separated by GPC with an acetate buffer (pH 5.0), and the fractions of TRITC-labeled thiol-introduced rHSA (TRITC-labeled SH-rHSA) were collected. The number of the SH groups conjugated to one rHSA molecule was determined by the quantification of the 2-thiopyridone (2-TP) at 343 nm that was liberated by the addition of DTT.

Preparation of rHSA-nanosheets

As shown in Figure 1, the substrate of the patterned ODS-SAM was immersed into an acetate buffer solution

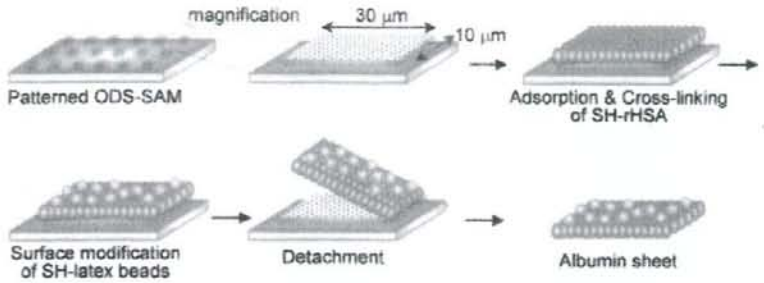

Figure 1. Preparation of free-standing rHSA-nanosheets having heterosurfaces on the patterned ODS-SAM. [Color figure can be viewed in the online issue, which is available at www.interscience.wiley.com.]

(pH 5.0) of the TRITC-labeled SH-rHSA at a concentration of 1 μg/mL for 1 h at r.t., and washed with an acetate buffer solution to remove the nonadsorbed SH-rHSA. The substrate was immersed into an acetate buffer solution containing copper ion (II) as a catalyst[25] at a concentration of 1 μM for 12 h at r.t. The series of adsorption, crosslinking, and washing processes were repeated three times. The substrate was immersed into a 1% (v/v) deca(oxyethylene) dodecyl ether ($C_{12}E_{10}$) solution at r.t. for 6 h, to obtain a free-standing rHSA-nanosheet suspension by releasing the rHSA-nanosheets from the substrate. We observed the resulting rHSA-nanosheets using an epifluorescence microscope (ECLIPS TE300, Nikon Co., Tokyo, Japan) equipped with a CCD camera, a confocal laser scanning microscope (LSM 510, Zeiss, Nikon Co.), and an atomic force microscope (AFM) at a tapping mode with a MFP-3D-BIO (Asylum Research, Co., Santa Barbara, CA).

Conjugation of NBD-labeled latex beads to the surface of rHSA-nanosheets

Latex beads (ϕ 100 nm) were mixed with an rHSA solution (50 mg/mL) and incubated at r.t. for 2 h to coat the surface of the latex bead with rHSA. After the separation of the free rHSA by ultracentrifugation (100,000*g*, 10 min, 4°C, twice), the rHSA-coated latex beads (rHSA-latex beads) were dispersed in a phosphate buffer solution (pH 7.4). The amount of rHSA adsorbed on the surface of the latex bead was analyzed by a microBCA kit (Pierce Biotechnology). A solution of LC-SPDP in DMSO (2 eq. mol with respect to the rHSA adsorbed on the surface of the latex bead) was added to the suspension of the rHSA-latex beads and incubated for 20 min at r.t. The solution of NBD in DMSO (2 eq. mol with respect to rHSA on the surface of the latex bead) was added to the suspension and incubated for 20 min at r.t. A DTT treatment (f.c. 20 mM) was carried out to reduce the PD groups to SH groups. The unreacted DTT and byproducts were separated by GPC, and the NBD-labeled thiol-bearing latex beads [SH-(NBD)latex beads] were collected.

On the other hand, the substrate of the TRITC-labeled rHSA-nanosheets was immersed in a phosphate buffer, and a DMSO solution of EMCS was added to the substrate and incubated for 20 min at r.t. to introduce maleimido groups on the nanosheet. The unreacted EMCS and byproducts were washed with a phosphate buffer, and the maleimido-bearing rHSA-nanosheets were obtained.

Finally, the SH-(NBD)latex beads were added to the maleimido-bearing rHSA-nanosheets, and incubated for 2 h at r.t. The unreacted SH-(NBD)latex beads and byproducts were washed with a phosphate buffer, and the rHSA-nanosheets, of which the obverse side was modified with the NBD-labeled latex beads, were observed using a confocal laser scanning microscope (LSM 510) and a Hitachi S-4500 field emission scanning electron microscope (SEM).

RESULTS

Water contact angle

The water contact angle of the substrate, which was coated with ODS-SAM, was estimated to be 83° ± 1° as listed in Table I. When the ODS-SAM-coated substrate was immersed into a phosphate buffer solution (pH 7.4) of rHSA at a concentration of 100 μg/mL, the water contact angle did not change (80° ± 2°). However, when the substrate was immersed in an acetate buffer solution (pH 5.0) of rHSA, the angle was significantly decreased to 67° ± 1°. The angle was restored to 82° ± 1° when the rHSA-treated substrate was immersed into a 1% (v/v) solution of $C_{12}E_{10}$ for 1 h. Therefore, we confirmed

TABLE I
Water Contact Angles of ODS-SAM Before and After rHSA Adsorption

rHSA Adsorption	Water Contact Angle (degree)
Before	83 ± 1
After	
pH 5.0	67 ± 1
pH 7.4	80 ± 2
$C_{12}E_{10}$[a]	82 ± 1

[a] $C_{12}E_{10}$ was added to the ODS-SAM after rHSA adsorption at pH 5.0, incubated at r.t. for 1 h and then washed with distilled water.

that rHSA molecules were adsorbed on the ODS-SAM at pH 5.0, and the adsorbed rHSA molecules were detached from the substrate by surfactant treatment.

Preparation of rHSA-nanosheets

We could not analyze the crosslinking ratio of the SH-rHSA molecules adsorbed on the ODS-SAM from quantification of the unreacted SH groups of the rHSA, because the amount of the adsorbed rHSA was below the detection limit. We explored the crosslinking of the SH-rHSA in an aqueous solution in order to determine the extent of crosslinking of the SH-rHSA on the ODS-SAM. We determined the number of SH groups bound to one rHSA molecule for mixtures of LC-SPDP and rHSA at 5, 7, and 10 mol/mol (mole equivalent of the rHSA concentration) ratios of LC-SPDP to rHSA. Based on the quantification of the 2-TP liberated by the addition of DTT, the number of SH groups bound to one rHSA molecule was estimated to be ~2.9 ± 0.8, 4.7 ± 1.1, and 7.4 ± 1.2 molecules, respectively. We oxidized the SH-rHSA molecules in the presence of copper ion (II) at r.t. and measured the degree of reaction by HPLC with a TSK-GEL G4000SW_{XL} column, by measuring the absorbance of the column effluent at 220 nm, which was attributed to the absorption of the amide linkage of rHSA. At pH 5.0, the three kinds of SH-rHSA having different numbers of SH groups were crosslinked, and the percentage of the peak area of the void fraction to the total peak, which corresponded to the amount of the crosslinked rHSA with a molecular weight of >670 kDa based on the elution time of thyroglobulin as a marker protein, was increased to 64, 75, and 96% with the increasing number of the SH groups bound to one rHSA molecule. All reactions were completed within 12 h. On the other hand, the three kinds of SH-rHSA were hardly crosslinked in the absence of copper ion (II) at pH 5.0 or in the presence of copper ion (II) at pH 7.4. Based on the earlier results, we decided that SH-rHSA molecules with 7.4 ± 1.2 SH groups bound to one rHSA molecule were to be crosslinked on the patterned ODS-SAM at pH 5.0 for 12 h in the presence of 1 μM copper ion (II).

Next, we explored the adsorption of SH-rHSA on the rectangle-patterned ODS-SAM regions. When the substrate of the patterned ODS-SAM was immersed in an acetate buffer solution (pH 5.0) of the TRITC-labeled SH-rHSA at a concentration of 1 μg/mL, the rectangular patterns (10 μm × 30 μm) were completely and selectively stained by the TRITC-labeled SH-rHSA as shown in Figure 2(a). After removing the nonadsorbed SH-rHSA by washing with the acetate buffer solution, we crosslinked the SH-rHSA molecules adsorbed on the patterned ODS-SAM following the aforementioned conditions, and immersed the substrate in a 1% $C_{12}E_{10}$ solution at r.t. for 6 h to detach the rectangles from the substrate. Next, we dropped the $C_{12}E_{10}$ solution containing the rectangular sheets onto a glass plate, and observed the surface of the plate using a confocal laser scanning microscopy. There were abundant rectangular rHSA-nanosheets in various conformations; in particular, the bent form of the rHSA-nanosheets was successfully observed in the three-dimensional images [Fig. 2(b,c)], demonstrating the flexible and tough nature of the rHSA-nanosheets.

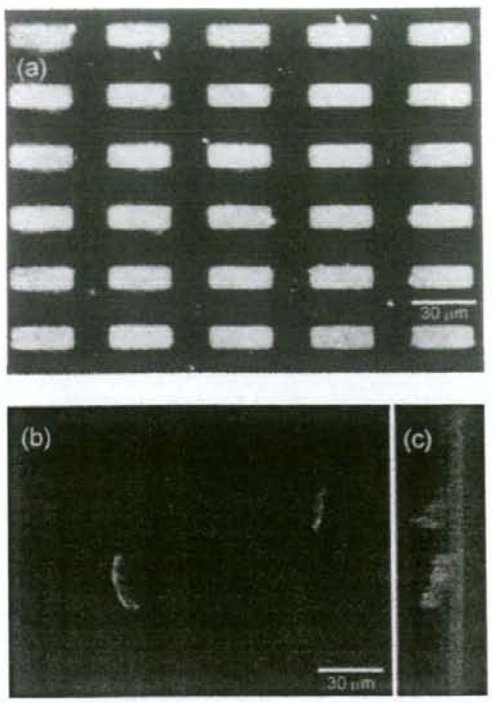

Figure 2. (a) Observation of SH-rHSA adsorbed onto the patterned ODS-SAM using fluorescent microscopy. (b) Observation of the free-standing rHSA-nanosheets detached from the patterned ODS-SAM and (c) the 90° rotation image of (b) using confocal laser fluorescent microscopy.

AFM analysis of rHSA-nanosheets

To establish the morphological detail and the thickness of the rHSA-nanosheets, the nanosheets on the patterned ODS-SAM were observed by AFM. Figure 3(a) shows a large-scale (90 μm × 90 μm), three-dimension AFM image of the rHSA-nano-